

# Investigation of Copper–Saccharide Complexation Reactions using Potentiometry and Electrospray Mass Spectrometry

Mona Shahgholi,<sup>1\*</sup> John H. Callahan,<sup>1</sup> Brian J. Rappoli<sup>1</sup> and David A. Rowley<sup>2</sup>

<sup>1</sup>Naval Research Laboratory, Chemistry Division, Code 6113, Washington, DC 20375, USA

<sup>2</sup>The George Washington University, Washington, DC 20052, USA

The associations between cupric ions and oligosaccharides of cellulose, chitin and chitosan were investigated using potentiometry and electrospray mass spectrometry. The goal of these studies was to understand the degree to which electrospray mass spectra reflect the solution chemistry of copper–oligosaccharide complexes. To this end, electrospray mass spectrometric data were compared with potentiometric studies. The potentiometric data revealed no copper binding for mono- and tetrasaccharides of cellulose and chitin, while the mass spectrometric data suggested the presence of distinct copper complexes, these attributed to charge attachment during desorption from the highly charged electrospray droplets. Difference in the distribution of tetrasaccharide–copper complexes for cellulose and chitin was attributed to possible differences in droplet solution conformations of these saccharides. For mono-, di- and tetrasaccharides of chitosan the potentiometric data showed strong copper complexation. For the tetrasaccharide the major species expected at pH 7 is a neutral copper complex. This neutral copper–tetrasaccharide complex was observed in the protonated form at relatively low abundances under high-voltage conditions in the electrospray interface. In this complex, Cu(II) is co-ordinated to the C(1)-alkoxide, the four amine nitrogens of chitosan tetrasaccharide and an anion. The ability of electrospray mass spectrometry to probe the immediate environment of the complex provides a clearer picture of the complex as it exists in solution, the associated counter-ions and possible differences in conformation. However, electrospray mass spectrometric data best reflect chemistries in highly charged droplets rather than systems at equilibrium, highlighting the significance of supporting techniques to fully understand a chemical system. © 1997 by John Wiley & Sons, Ltd.

*J. Mass Spectrom.* 32, 1080–1093 (1997)

No. of Figures: 11 No. of Tables: 1 No. of Refs: 40

KEYWORDS: metal complexation; electrospray mass spectrometry; potentiometry; carbohydrates

## INTRODUCTION

The ability of organic molecules to bind metal ions is important biologically, environmentally and industrially.<sup>1</sup> Bioavailability of metals and metal toxicities to organisms are influenced strongly by the presence of chelators.<sup>2,3</sup> Chelating ligands can also influence the geochemical cycling of metals in the environment when present in high concentrations.<sup>4</sup> Metal–biomolecule associations are particularly significant in marine environments where metal ion bioavailability or toxicity is directly influenced by the presence of ligands.<sup>1</sup> For example, metal complexation by free or attached carbohydrates (polysaccharide mats on ocean floors) can alter free metal ion availability or create locally toxic environments.<sup>5</sup> Metal–ligand interactions also have implications in marine surface biofouling and bioremediation, the latter depending directly upon the metal-binding affinities and selectivities of chelating molecules.<sup>5</sup>

Metal–ligand associations have been routinely studied with the aid of X-ray crystallography,<sup>6a</sup> nuclear magnetic resonance (NMR) spectroscopy, electron spin resonance spectroscopy and electrochemical techniques, providing information regarding binding sites and binding affinities.<sup>6b</sup> Other techniques, such as graphite furnace atomic absorption spectroscopy, inductively coupled plasma mass spectrometry and glow discharge mass spectrometry, have also been used for analysis of metal–ligand complexes, only providing information with respect to the identities and amounts of metals.<sup>7</sup>

More recently, electrospray ionization mass spectrometry (ESMS)<sup>8</sup> has been used for the study of metal–ligand complexes because of the potential for examining both metal and ligand components simultaneously. The appeal of ESMS for investigation of metal complexation reactions principally stems from its inherent ‘softness’ which allows transfer of ‘intact’ complexes from the condensed phase to the gas phase. This property is essential for examination of metal complexes since it preserves the chemical identity of the solutes and the specificity of the associations in the solution. An additional feature of electrospray ionization (ESI) is the ability to analyze complexes with multivalent metal ions. Prior to ESMS, singly charged, and occasionally

\*Correspondence to: Naval Research Laboratory, Chemistry Division, Code 6113, Washington, DC 20375, USA.  
Contract sponsor: Office of Naval Research.

doubly charged, metal ion–ligand complexes had been observed by fast atom bombardment,<sup>10</sup> thermospray<sup>11</sup> and electrospray ionization;<sup>12</sup> however, none was as successful as ESI in transferring the multiply charged metal–ligand species from solution to gas phase.<sup>8a</sup> Finally, ESMS has been suggested to be an accurate probe of solution equilibria, responding to changes in solution pH, presence of various counterions, metal:ligand ratios, another feature directly relevant to investigations of complexation reactions.

Some studies dealing with metal–ligand interactions have focused on the various features that render ESMS so desirable and useful. For example, Colton and co-workers applied ESMS to examination of ligand exchange reactions for Cu(I)-tetrahydroborate species<sup>9</sup> and methylphosphonium cations.<sup>13</sup> These studies demonstrated that labile complexes responded strongly to nozzle–skimmer voltages owing to collisional decomposition in the electrospray ion source, but non-labile complexes yielded intact ions which correlated directly with their solution composition. Kebarle and co-workers used ESMS to study ion–ligand and ion–solvent interactions for doubly and triply charged metal ions which previously were inaccessible to other ionization techniques.<sup>14</sup> Gas phase charge reduction reactions were noted to compete with dissociation reactions (ligand loss) as the second ionization energy of the metal increased.<sup>14b</sup> Cheng *et al.* studied aqueous solutions of metal salts by ESMS, focusing on correlations between solution equilibria and mass spectrometric results.<sup>15</sup> Their studies indicated a strong semi-quantitative agreement between mass spectrometric data and calculated species equilibrium solution concentrations. Discrepancies were attributed to differences in the desorption efficiencies of various species.

Other studies, using systems with well-characterized solution chemistries, have attempted to determine the appropriate ESMS experimental conditions for observation of the metal–ligand complexes. For example, Fenselau and co-workers used ESMS to assess the complexation of zinc and cadmium ions by metallothioneins.<sup>16</sup> Complexes of metallothioneins with seven-co-ordinated divalent metal ions were detected when care was taken to use pH values that maintained native co-operative binding in the proteins. Similarly, Loo and co-workers used ESMS to determine metal stoichiometries for calcium-binding proteins.<sup>17</sup> They emphasized the importance of metal ion concentrations and selection of ionization polarity in preserving specific metal–protein associations and reducing the likelihood of observing non-specific metal attachment respectively. Van Berkel *et al.* investigated the complexation of porphyrins with di- and trivalent metal ions using ESMS.<sup>18</sup> They reported the formation of metal–porphyrin radical cations for divalent metal ions and stressed the role of solvent composition in condensed phase ionization mechanisms known for metal–porphyrins, namely protonation, sodiation and charge transfer.

Finally, unique capabilities of ESMS for the study of metal–ligand complexes have been shown in numerous reports. For example, metal speciation using ESMS was reported by Gatling *et al.* in a study of Cu(I) and Cu(II) complexes present in jet fuel.<sup>19</sup> The nature of the Cu

species detected by ESMS was found to depend on the nitrogen and oxygen ligands introduced during the analysis or present in the carrier stream. Loo and Hu investigated the interaction of histidine-containing peptides and  $\text{Zn}^{2+}$ ,  $\text{Ni}^{2+}$ ,  $\text{Co}^{2+}$  and  $\text{Cu}^{2+}$  metal ions by ESMS.<sup>20</sup> CAD spectra of the gas phase  $\text{Zn}^{2+}$ –,  $\text{Co}^{2+}$ – and  $\text{Ni}^{2+}$ –peptide complexes showed nearly exclusive dissociation at histidine sites, thereby suggesting metal binding at or near histidine residues.<sup>20</sup> CAD spectra of the gas phase  $\text{Cu}^{2+}$ –peptide complexes showed a different fragmentation pattern which suggested metal binding at the carboxylate terminus of the peptide.<sup>20</sup> Van Dorsselaer *et al.* demonstrated the ability of detecting myohemoglobin complexes using ESMS if the pH, ionic strength, temperature and nozzle–skimmer voltage were carefully controlled.<sup>21</sup> The metal center of the complex was released when the voltage difference between the nozzle and skimmer elements was increased.

These studies collectively suggest that ESMS is indeed a powerful technique for probing metal–ligand interactions in the condensed phase. It is also evident that more remains to be discovered about the processes of ESI and how they affect the examination of metal–ligand interactions. To date, a key question still involves the extent to which solution equilibria are reflected in the mass spectra, i.e. is it possible to differentiate between complexes present in the bulk solution, those formed in the gas phase by ion–molecule reactions and complexes generated during the desorption process? Although some studies have indicated that ESI spectra approximate solution equilibria, these cases have largely involved complexes with large formation constants, as is the case in many protein–metal interactions. However, where other types of biomolecules are concerned, it is not clear that solution equilibria are accurately reflected in every case. This is of particular concern in this study, as it aims to address the feasibility of using ESI to probe metal ion interactions with less well-studied biomolecules, such as carbohydrates. Among the variety of molecules present in marine environments, carbohydrates comprise an important group of potential ligands because of their high natural abundances and various affinities for binding metal ions.

The studies described here have focused on establishing whether ESI spectra can accurately probe the metal-binding capabilities of carbohydrates in the marine environment. To this end, the metal-binding properties of model carbohydrates, mono- and oligosaccharides of chitosan, chitin and cellulose (Fig. 1), were investigated. Chitosan is a linear homopolymer of  $\beta$ -1,4-linked D-glucosamine residues possessing high selectivities for transition metal ions. 'Chitin' refers to the acetylated form of chitosan, consisting of  $\beta$ -1,4-linked N-acetyl-D-glucosamine and possessing significantly lower metal-complexing affinities.<sup>22</sup> Literature reports often refer to chitin as a potent chelating polymer because essentially all forms of naturally occurring chitin are partially deacetylated and therefore exhibit some affinity for complexing transition metal ions. In this work however, the term 'chitin' refers to the fully acetylated polymer for which the copper-binding affinity is undetermined. Owing to their abundance in the marine environment, chitosan and chitin can control

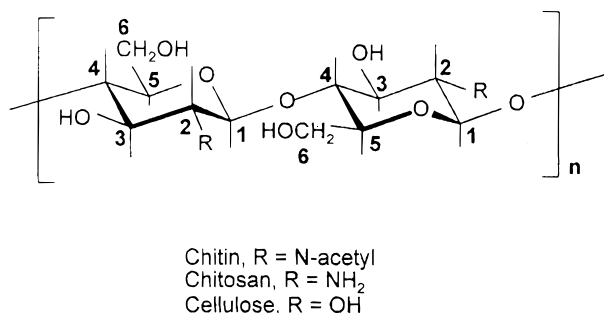


**Figure 1.** Schematic diagram showing structures of chitin, chitosan and cellulose. Substituent R on C(2) of each hexose monomer is a hydroxyl group in cellulose, an amino group in chitosan and an *N*-acetyl group in chitin.

metal ion equilibria in their surroundings, influencing metal ion bioavailability and toxicities.<sup>22</sup> Specifically, chitin and chitosan have been shown to be highly effective in reducing the bioavailability of copper to marine biota, this attributed to their tenacity for binding copper.<sup>23</sup> Furthermore, since elevated levels of copper released to the environment are toxic to aquatic organisms,<sup>24</sup> the copper-binding affinity of chitin is also important in regulating copper toxicity. Cellulose, the major polysaccharide in plant cell walls (although it is also present in a few bacteria and fungi, most algae and some animals<sup>25</sup>), was chosen as a benchmark for these studies. Cellulose consists of  $\beta$ -1,4-linked D-glucose residues, differing from chitosan and chitin in the C(2) position of these hexose monomers, which bears a hydroxyl group rather than an acetamide or amino group. Because of the absence of nitrogen, which is often involved in strong binding of transition metal ions, cellulose was expected to have weaker metal-ligand interactions than chitosan or chitin.<sup>26</sup>

The interactions of these model oligosaccharide and copper ions were studied by electrospray mass spectrometry. The results were compared with potentiometric measurements of solution equilibria, which were determined for mono- and tetrasaccharides of cellulose and chitin and for mono-, di- and tetrasaccharides of chitosan. These data were previously not available in the literature. The results of these studies revealed cases where the data from the two techniques converge and cases where the data do not agree. Consequently, the picture of the electrospray process that emerges does not appear to be a simple dichotomy between 'solution' and 'gas phase.' Instead, as others have noted, ESI spectra appear to reflect a complex convolution of shifting equilibria induced by droplet evaporation.<sup>27</sup> These studies are critical not only in enhancing our understanding of ESMS but also in determining the feasibility of using ESMS for determining metal-ligand equilibria.

## EXPERIMENTAL

### Potentiometric Studies

Potentiometric measurements were made with an Orion 720A meter using a Ross pH electrode or an Orion

cupric ion-selective electrode (ISE) with an Ag/AgCl double-junction reference electrode. Freshly prepared deionized water was obtained using a Millipore Milli-Q plus system. Reagent grade KNO<sub>3</sub> and (CH<sub>3</sub>)<sub>4</sub>NClO<sub>4</sub> were recrystallized from deionized water. Reagent grade EDTA was recrystallized from ethanol/water. Cu(NO<sub>3</sub>)<sub>2</sub> · 6(H<sub>2</sub>O) (Aldrich Chemical Co., Milwaukee, WI), chitobiose hydrochloride, chitotetrasaccharide hydrochloride (YSK, Tokyo, Japan), D(+)-glucosamine, D(+)-glucose, *N*-acetyl-D-glucosamine and potassium acid phthalate (Sigma Chemical Co., St. Louis, MO) were used as received. Potentiometric titrations were conducted in a glass-jacketed titration cell at 25.00 ± 0.05 °C. Titrant was delivered using a 10 ml capacity Metrohm 665 piston buret. Air was excluded from the titration cell by purging with argon. The ionic strength of all solutions was adjusted to 0.100 M with KNO<sub>3</sub> or to 0.050 M with (CH<sub>3</sub>)<sub>4</sub>NClO<sub>4</sub>. Carbonate-free KOH solutions were prepared using Acculute volumetric concentrates and standardized by titration against KHP. The pH electrode was calibrated such that p[H<sup>+</sup>] was measured. Copper(II) solutions were standardized by titration with EDTA using a cupric ISE to measure the endpoint. Ligand protonation and metal-binding constants were calculated from equilibrium potentiometric data with the use of the programs BEST and PKAS.<sup>28</sup> Species distribution curves were calculated with the use of the program COMICS.<sup>29</sup>

### Mass Spectrometric Studies

The experiments were performed on a TSQ-70 triple-quadrupole mass spectrometer (Finnigan-MAT Corp., San Jose, CA) fitted with an electrospray source. This source employs heat for desolvation of electrosprayed droplets and a flow of sheath gas and auxiliary gas to assist in droplet formation and evaporation of less volatile solvents. Special features of this source are the presence of a tube lens in the capillary (nozzle)-skimmer region and an RF-only octapole beyond the skimmer. The tube lens is used to focus ions and pass them through a grounded skimmer positioned off-axis with respect to the nozzle. Increasing the voltage difference between the nozzle and the skimmer ( $\Delta V$ ) has been used to induce fragmentation (collision-activated dissociation, CAD) and to assist in further desolvation of electrosprayed droplets by increasing ion collisions with neutral gas in the expansion region.<sup>30</sup> No precursor ions are selected in this in-source CAD, in contrast with traditional CAD where a precursor ion is selected and admitted into a high-pressure atmosphere of an inert gas for dissociations. In the Finnigan interface, in-source CAD is effected by manipulating  $\Delta V$  between the heated capillary and the tube lens. Extreme changes in  $\Delta V$  also influence the ion transmission properties of the source and therefore the observed abundances of the ions (see below).

All electrospray samples were prepared using 1:1 (v/v) methanol:water. Methanol was of HPLC grade (Fisher Scientific, Pittsburgh, PA) and water distilled and deionized. The electrospray voltage was typically set at 4.7 kV. Samples were infused directly (without an

additional liquid sheath) at  $2 \mu\text{L min}^{-1}$  using a Model 22 Harvard syringe pump (Harvard Apparatus Inc., Natick, MA). The mass spectrometer was initially tuned by infusing a standard solution of  $20 \text{ pm } \mu\text{L}^{-1}$  of the tetrapeptide methionyl-arginyl-phenylalanyl-alanine (MRFA) (Sigma Chemical Co., St. Louis, MO) and  $5 \text{ pm } \mu\text{L}^{-1}$  myoglobin (Sigma Chemical Co., St. Louis, MO) in 0.25% acetic acid. Following tuning and mass calibration with the MRFA-myoglobin solution, appropriate ES conditions for analysis of the sugar-metal complexes were determined empirically. A standard mixture of chitin oligosaccharide,  $20 \mu\text{M}$  in chitobiose (Sigma Chemical Co., St. Louis, MO), chitotrisaccharide, chitotetrasaccharide, chitopentasaccharide and chitohexasaccharide (YSK Tokyo, Japan) was prepared in  $25 \mu\text{M NaI}$ . These sugars appear as sodium adducts under standard ES conditions. High temperatures and large  $\Delta V$  result in observation of sugar dehydration products ( $[\text{M} + \text{Na}^+ - \text{H}_2\text{O}]^+$ ) and cleavage of the glycosidic bonds. Very low capillary temperatures and low  $\Delta V$  result in lowered abundances and appearance of solvent clusters and clustered molecular ions. To create gentle desorption conditions for the analysis of the sugar-metal complexes, the capillary temperature and  $\Delta V$  were lowered until the first appearance of solvated molecular ions. The capillary temperature was typically set at  $180^\circ\text{C}$  and  $\Delta V$  at approximately 40 V.  $\Delta V$  was changed over a range of 60 V (from 20 to 80 V) in a set of voltage change experiments used for monitoring copper-chitosan complexes. For these experiments,  $\Delta V$  effects on ion transmission were examined by electrospraying a  $50 \mu\text{M}$  solution of chitotetrasaccharide and monitoring the absolute abundances of  $(\text{M} + \text{Na})^+$  at  $m/z$  853. The signal-to-noise (S/N) ratio for  $m/z$  853 improved by a factor of four as  $\Delta V$  was increased from 20 to 80 V. This improvement in S/N was kept in mind during analysis of data acquired under high- $\Delta V$  conditions; however, data were not corrected for differences in desorption efficiencies of the various species and  $\Delta V$  effects on ion transmission remain strictly qualitative in nature.

CAD experiments were performed for structural identification using argon as a collision gas at a pressure of  $(2.4\text{--}2.6) \times 10^{-3}$  Torr with collision energies ranging between 20 and 40 V. During these experiments the pressure in the mass analyzer was approximately  $3 \times 10^{-5}$  Torr. Mass spectra were generally acquired over  $m/z$  100–1200 at 1.5 scans per second. Spectra presented are the sums of 10–14 scans.

## RESULTS AND DISCUSSION

Complexation of sugars and transition metal ions in solution has been traditionally examined with the aid of NMR, electrophoretic and potentiometric methods focusing on determination of conformational features required for complexation, the stability constants of the complexes and their structures.<sup>26</sup> These studies have determined that metal binding for neutral sugars is strongly controlled by the conformation of the sugar and the size of the cation.<sup>26</sup> Optimal binding is noted for sugars with a contiguous sequence of *axial*, *equato-*

*rial*, *axial* hydroxyl groups and cations with radii in the 100–110 pm range, although some complexation may still be possible for cations with radii outside the specified range and for other sugar conformations.<sup>26</sup> For aminosugars, such as the chitosan saccharides under investigation, metal binding is predominantly controlled by the nitrogen atom and the co-ordinating metal. Presence of a hydroxyl group adjacent to the nitrogen atom is suggested to favor the formation of bidentate complexes that are stronger relative to the nitrogen-free sugars.<sup>26</sup>

Cellulose, chitin and chitosan are structurally very similar<sup>22,25</sup> in that all their hydroxyl groups occupy equatorial positions, resulting in an unfavorable conformation for metal complexation. Thus, with regard to the association between cupric ions and cellulose, chitin and chitosan saccharides investigated in this study, complexation was expected to be negligible with cellulose and fully acetylated chitin saccharides (neutral sugars) because of their all-*equatorial* conformation and cupric ions' non-optimal atomic radius (72 pm);<sup>31</sup> however, cupric ions were expected to be more strongly complexed by chitosan owing to the presence of the primary amine on C(2) of the hexose ring,<sup>26</sup> in spite of the all-*equatorial* conformation. Moreover, there is significant evidence from other studies that chitosan is a strong binding ligand.<sup>22,23</sup>

Mass spectrometric studies of carbohydrate-transition metal ion associations are limited and primarily focus on determination of appropriate MS experimental conditions and CAD of the complexes detected in the gas phase. For example, various mono- and disaccharides were examined by ESMS for their metal-binding affinities for a number of alkali, alkali earth and transition metal ions.<sup>33a</sup> Binding of Cu and Ni to chitin oligosaccharides was examined by both ESMS and matrix-assisted laser desorption time-of-flight mass spectrometry, noting differences in the nature of the information provided by each technique and discussing the fragmentation patterns of the transition metal-sugar adducts.<sup>33b</sup> The binding of alkali, alkali earth and cobalt ions to a number of sugars was examined by Leary and co-workers, focusing on the fragmentation patterns of these sugar-metal adducts.<sup>34</sup> Leary and co-workers further investigated the interaction of first-row transition metals with a trisaccharide and a pentasaccharide, focusing on criteria that would enhance the formation of metal-oligosaccharide adducts and their subsequent tandem mass spectrometric analysis.<sup>31</sup> Copper-sugar complexes were produced with greater difficulty (relative to  $\text{Ca}^{2+}$ ,  $\text{Co}^{2+}$  and  $\text{Mn}^{2+}$ -sugar complexes) and their tandem mass spectra were also less structurally informative.<sup>31</sup>

By analogy with the metal-ligand studies alluded to earlier, ESMS analysis of metal-carbohydrate complexes is also expected to be governed by solution parameters, such as pH, nature of the solvent and ionic strength, and instrumental parameters, mainly the temperature of the heated electrospray capillary and  $\Delta V$  between the nozzle and skimmer elements. The pH and nature of the solvent are important in ensuring the stability of the metal adducts in the ES solvent,<sup>35</sup> while the operating voltages in the ES source are critical in detection of intact metal adducts. The temperature of the

heated capillary is particularly important in carbohydrate analysis, since these species are thermally labile and easily undergo dehydration reactions at high temperatures.

#### Associations between cello- and chitosaccharides and cupric ions

The mass spectrometric samples consisted of 50  $\mu$ M tetrasaccharide and 0, 10, 30, 50, 100 and 200  $\mu$ M copper nitrate, always prepared immediately prior to the mass spectrometric analysis in order to ensure analyte stability. The pH of samples in the 1:1 (v/v) methanol:water solvent was approximately 7. It should be noted that pH values in mixed solvents differ slightly from those reported for aqueous solutions; addition of methanol is reported to result in a higher pH.<sup>36</sup>

Several distinct sugar-copper complexes were observed while testing for copper binding by cellotetra-saccharide using a solution of 50  $\mu$ M sugar and 100  $\mu$ M copper:  $[M + Cu]^{2+}$  at  $m/z$  365,  $[M_2 + Cu]^{2+}$  at  $m/z$  698,  $[M - H + Cu]^+$  at  $m/z$  728,  $[M + CuNO_3]^+$  at  $m/z$  791 and  $[M_3 + Cu]^{2+}$  at  $m/z$  1031 (see Fig. 2). Other prominent copper complexes detected were  $m/z$  126, 158 and 190 attributed to  $[Cu(OCH_3)CH_3OH]^+$ ,  $[Cu(OCH_3)(CH_3OH)_2]^+$  and  $[Cu(OCH_3)(CH_3OH)_3]^+$  respectively. Similar species were observed when the copper complexation affinity of chitotetra-saccharide was tested by ESMS. The complexes observed for a solution of 50  $\mu$ M chitotetra-saccharide and 100  $\mu$ M copper were  $[M + Cu]^{2+}$  at  $m/z$  447,  $[M_2 + Cu]^{2+}$  at  $m/z$  862 and  $[M - H + Cu]^+$  at  $m/z$  892 (see Fig. 3).

As noted above, the copper complexes observed with cellotetra-saccharide and chitotetra-saccharide were similar in nature. However, the relative abundances of the species observed at each copper concentration differed between the two tetrasaccharides. For example,  $[M + Cu]^{2+}$  was the most abundant complex for chitotetra-saccharide over the range of Cu(II) concentrations tested, while  $[M_2 + Cu]^{2+}$  typically predominated in the spectra of cellotetra-saccharide. The observed differences in the distribution of the copper-oligosaccharide species for the two tetrasaccharides is not related to their solution equilibria, as evidenced from examination of their potentiometric data which showed no evidence for the formation of copper-cellotetra-saccharide and copper-chitotetra-saccharide complexes. For the potentiometric studies the association of Cu(II) with glucose, acetyl-glucosamine, cellotetra-saccharide and chitotetra-saccharide was measured using a cupric ISE with  $(CH_3)_4NClO_4$  as a supporting electrolyte. This electrolyte was used to avoid competing cation-saccharide associations.<sup>37</sup> The potentiometric measurements were conducted at  $p[H^+] = 4$  to 4.5 to ensure that copper hydroxide species were not formed. Typical solutions were 7.5 mM in ligand for the monosaccharides and 0.5 mM in ligand for the tetrasaccharides. Ligand:metal ratios ranged from 30:1 to 1:1. Under the conditions of this study, titration curves for copper only yielded free  $Cu^{2+}$  concentrations that could be explained by dilution curves, i.e. no association of Cu(II) was observed. Similar studies were also carried out at higher  $p[H^+]$  values and there was no evidence of copper-oligosaccharide complex formation under the more basic conditions.

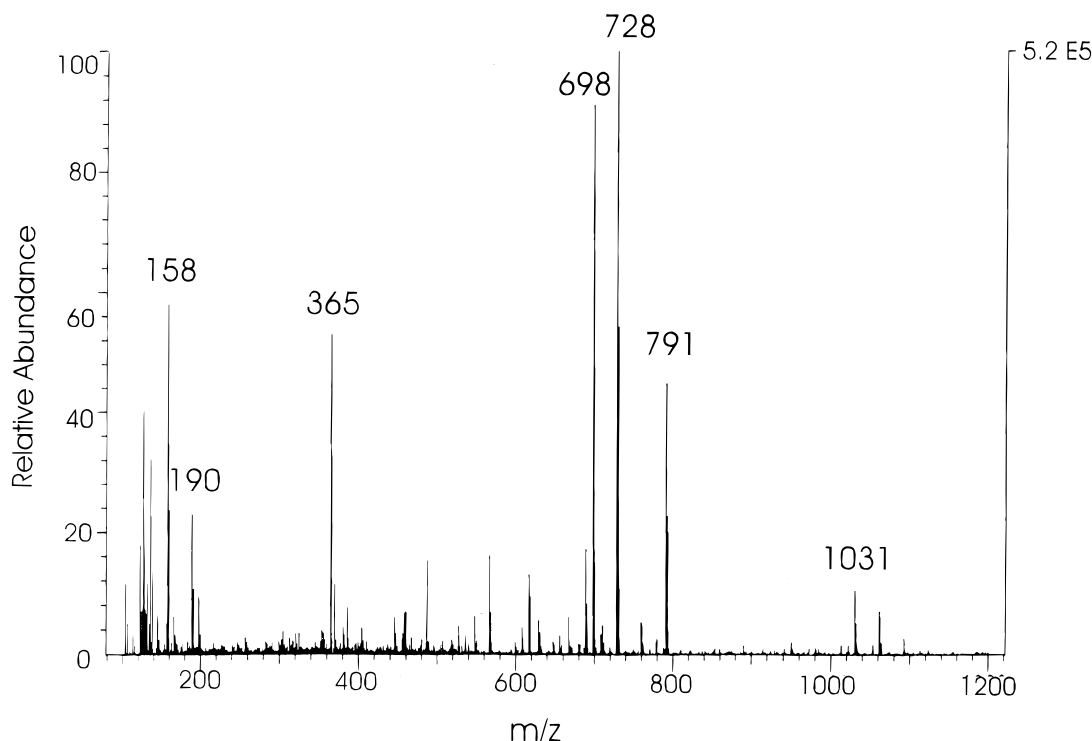


**Figure 2.** ES mass spectrum of 50  $\mu$ M cellotetra-saccharide and 100  $\mu$ M copper nitrate in 1:1 (v/v) methanol:water, pH  $\approx$  7. Copper-saccharide complexes observed were  $[M + Cu]^{2+}$  at  $m/z$  365,  $[M_2 + Cu]^{2+}$  at  $m/z$  698,  $[M - H + Cu]^+$  at  $m/z$  728,  $[M + CuNO_3]^+$  at  $m/z$  791 and  $[M_3 + Cu]^{2+}$  at  $m/z$  1031. Species with  $m/z$  126, 158 and 190 are attributed to  $[Cu(OCH_3)CH_3OH]^+$ ,  $[Cu(OCH_3)(CH_3OH)_2]^+$  and  $[Cu(OCH_3)(CH_3OH)_3]^+$  respectively. Absolute abundances are shown in the upper right corner of the figure.

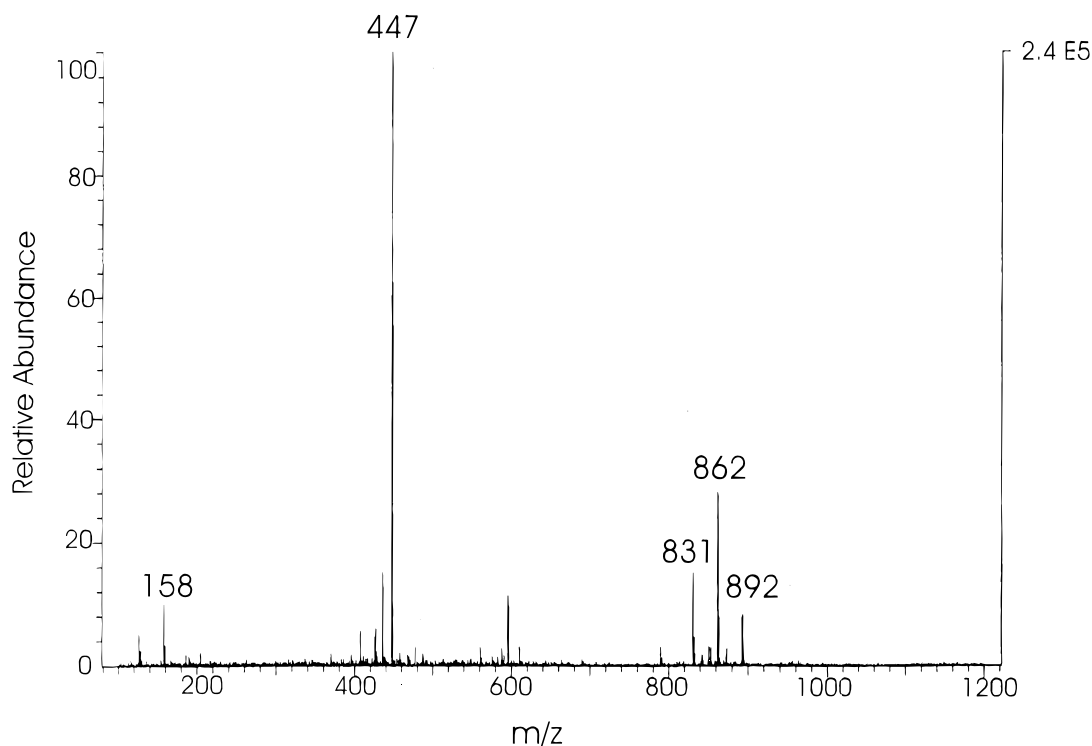


**Figure 3.** ES mass spectrum of 50  $\mu\text{M}$  chitotetrasaccharide and 100  $\mu\text{M}$  copper nitrate in 1:1 (v/v) methanol:water, pH  $\approx$  7. Copper-saccharide complexes were  $[\text{M} + \text{Cu}]^{2+}$  at  $m/z$  447,  $[\text{M}_2 + \text{Cu}]^{2+}$  at  $m/z$  862 and  $[\text{M} - \text{H} + \text{Cu}]^+$  at  $m/z$  892. Absolute abundances are shown in the upper right corner of the figure.

Mass spectrometric observation of such species in the absence of equivalent condensed phase complexes suggested that cationization (Cu adduction) of tetrasaccharides had occurred during desorption from the charged droplets or following desorption in the gas phase. It seems unlikely that gas phase reactions could be responsible for the formation of the observed complexes, as the volatility of the oligomers is low and there was no significant dependence of complex abundance on the magnitude of  $\Delta V$ , the voltage difference between the heated capillary and the tube lens. The possibility that chemistry in the charged droplet plays a role seems more likely, as suggested by Fenn's<sup>27</sup> extension to the ion evaporation model of Iribarne and Thomson.<sup>38</sup> According to this model, the positively charged ES droplets carry an excess of charge on their surface, a portion of which is carried by  $\text{Cu}^{2+}$  ions. During droplet evaporation the oligosaccharides spend some time in the vicinity of the shrinking droplet, whose surface charge density continues to increase until it reaches the Rayleigh limit for explosion of ion evaporation. In this highly charged surface region,  $\text{Cu}^{2+}$ -tetrasaccharide interactions, governed to a large extent by ion-dipole interactions, lead to charge attachment and desorption of copper-tetrasaccharide complexes that were not present in bulk solution. In this model the conformation of the saccharide at the droplet surface and its relative hydrophobicity are expected to influence charge attachment and the nature of complexes observed. Thus, in ESMS analysis of chitotetrasaccharide and cellotetrasaccharide, droplet solution conformations are probably different owing to the size and nature of the C(2) substituents. The bulkier and more hydrophobic acetylated amino group at C(2) of chito-

tetrasaccharide, compared with the hydroxyl group at C(2) of cellotetrasaccharide, may sterically control the extent of multimer formation (species such as  $[\text{M}_2 + \text{Cu}]^{2+}$  and  $[\text{M}_3 + \text{Cu}]^{2+}$ ) or affect the solvation properties of the molecule and charge attachment. These effects are complex and require further examination.

With respect to the goals of this work, mass spectrometric observation of Cu-cellotetrasaccharide and Cu-chitotetrasaccharide adducts in the absence of equivalent solution complexes is significant because it shows that ESMS does not entirely reflect solution equilibria and highlights the need for supporting techniques for data interpretation. Probably, it is more appropriate to state that ESMS data reflect charged droplet chemistry, this suggested by the observed changes in the relative abundances of the desorbed complexes as a function of copper concentrations. Furthermore, the differences in the distribution of copper-chitotetrasaccharide and copper-cellotetrasaccharide complexes possibly indicate differences in solution conformation that can be potentially probed by ES mass spectrometry, a subject of further study in this laboratory.

#### Associations between chitosan saccharides and cupric ions

In contrast with cellotetrasaccharide and chitotetrasaccharide, the chitosan tetrasaccharide was expected to bind copper effectively using the free amine groups on the C(2) position of each monomer.<sup>32</sup> To test the copper-binding affinity of the chitosan tetrasaccharide

(denoted as C4san hereafter), solutions consisting of 40  $\mu\text{M}$  C4san with 0, 10, 30, 50, 100 and 200  $\mu\text{M}$  of copper nitrate were prepared and examined by ESMS. As before, the pH of these samples was approximately 7. A typical mass spectrum of C4san with added copper is presented in Fig. 4. The main species noted in the mass spectrum were the doubly protonated C4san,  $[\text{M} + 2\text{H}^+]^{2+}$ , at  $m/z$  332, low abundances of a glycosidic cleavage ion,  $m/z$  502, and minor amounts of the singly protonated C4san species at  $m/z$  663. Based on the previously noted lack of agreement between ESMS data and solution equilibrium measurements, this observation suggested that the expected Cu–C4san complexes were not observed by ESMS under the operating mass spectrometric conditions. A possible explanation is that neutral Cu–C4san complexes are formed in solution. A similar formation of neutral metal–ligand complexes has also been suggested by Gatlin and Turecek in their investigation of copper complexation with amino acids.<sup>39</sup> To test the possibility that undetected Cu–C4san complexes were formed, the intensity of  $[\text{M} + 2\text{H}^+]^{2+}$  ( $m/z$  332) was measured as a function of  $[\text{Cu}^{2+}]$  in order to monitor changes in the solution concentrations of the free C4san (Fig. 5A). A steady decline in the relative abundances of  $m/z$  332 was noted as  $[\text{Cu}^{2+}]$  was increased, suggesting removal of free C4san by complexation to cupric ions. Since high solution ionic strengths and competition between analyte ions and cupric ions for ion desorption<sup>40</sup> also result in lowered ES sensitivity, the experiment was repeated with NaI (400  $\mu\text{M}$ ) in place of copper nitrate (Fig. 5B). Under these conditions no decline in response was observed, suggesting that changes in solution ionic strengths or competing ion desorption processes<sup>40</sup> could not be responsible for the declining abundances

of the protonated C4san. These results suggest the formation of neutral and/or negatively charged Cu–C4san complexes not detectable in the positive ion mode.

The formation of neutral copper–C4san complexes at  $\text{pH} \approx 7$  was indeed supported by the following potentiometric experiments aimed at determination of the conditional stability constants for complexation of copper by chitosan saccharides. These studies were initially performed for glucosamine hydrochloride and chitosan disaccharide (C2san) hydrochloride to help elucidate the behaviour of the more complex chitosan tetrasaccharide (C4san) hydrochloride. Measurement of conditional stability constants requires the measurement of protonation constants as a preliminary step, since the equilibrium measurement involves the competitive binding of protons and cations at basic moieties. The protonation constants of glucosamine hydrochloride, C2san hydrochloride and C4san hydrochloride were measured using a pH electrode with  $\text{KNO}_3$  as a supporting electrolyte. Typical solutions were 2.0 mM in ligand. The hydrochloride salts of glucosamine, C2san and C4san were defined as  $\text{MH}^+$ ,  $\text{MH}_2^{2+}$  and  $\text{MH}_4^{4+}$ , since they behave as di-, tri- and penta-protic acids (protons are dissociable from the amino and C(1) hydroxyl moieties) under the conditions of our study. Plots of  $a$  versus  $\text{p}[\text{H}^+]$  ( $a$ , moles of base added per mole of carbohydrate) showed a steep inflection at  $a = 1, 2$  and  $4$  for  $\text{MH}^+$ ,  $\text{MH}_2^{2+}$  and  $\text{MH}_4^{4+}$  respectively. The values of  $K_1$  were estimated since the  $\text{p}[\text{H}^+]$  was too high to be measured accurately in this region by potentiometry.  $K_1$  was assigned to the C(1) hydroxyl group, while  $K_2$  through  $K_5$  were assigned to the protonation of the amino groups. The first protonation constant was considerably higher than the subsequent protonation constants owing to the high

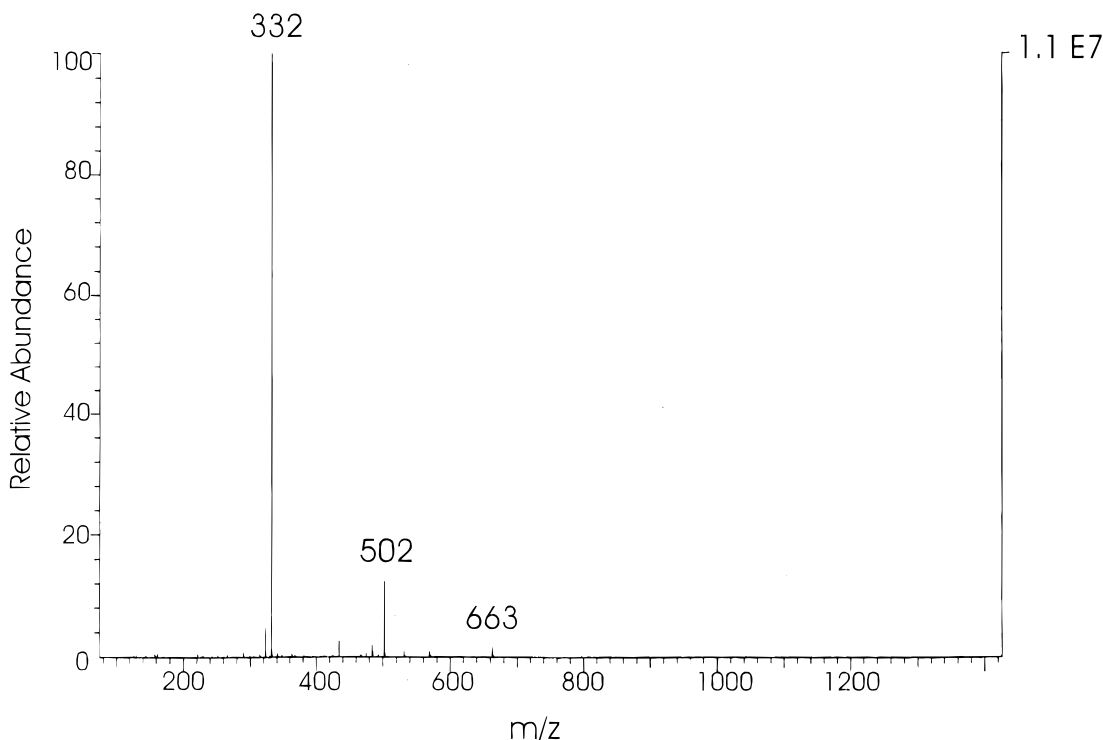


**Figure 4.** ES mass spectrum of 40  $\mu\text{M}$  chitosan tetrasaccharide (C4san) and 200  $\mu\text{M}$  copper nitrate in 1 : 1 (v/v) methanol : water,  $\text{pH} \approx 7$ .  $[\text{M} + 2\text{H}^+]^{2+}$  was detected at  $m/z$  332 and  $[\text{M} + \text{H}^+]^{2+}$  at  $m/z$  663. A glycosidic cleavage product ion was detected at  $m/z$  502. Absolute abundances are shown in the upper right corner of the figure.

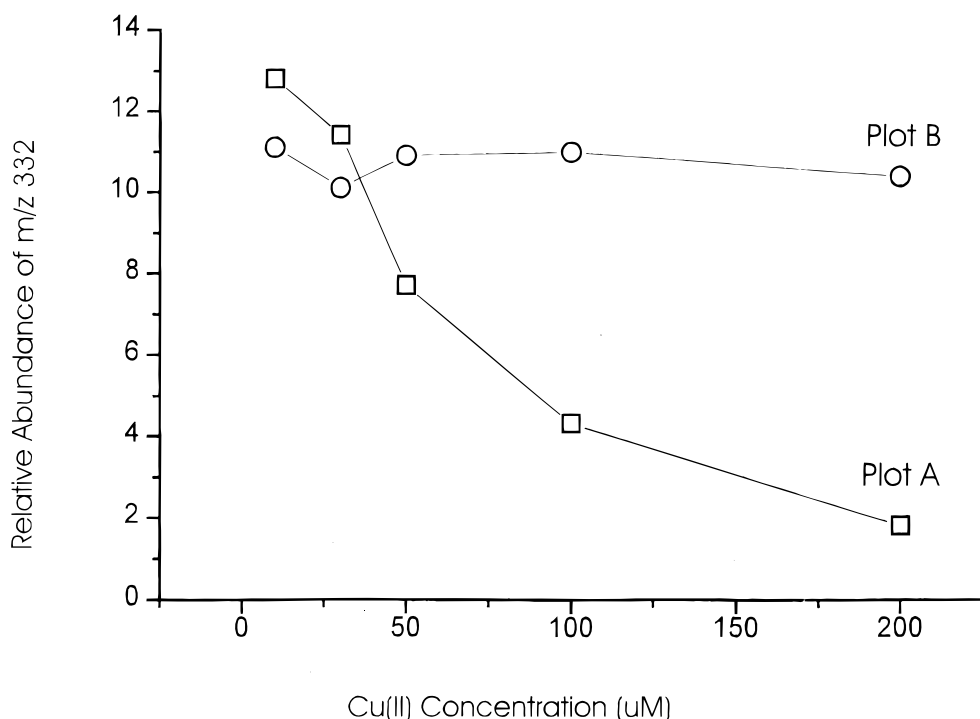


**Figure 5.** Relative abundances of 40  $\mu\text{M}$  chitosan tetrasaccharide,  $[\text{M} + 2\text{H}^+]^{2+}$ , monitored at  $m/z$  332, as a function of copper nitrate (A) and sodium iodide (B) concentrations (10–200  $\mu\text{M}$ ). Solutions were prepared in 1:1 methanol: water, pH  $\approx$  7.

basicity of the hydroxyl oxygen. The protonation constants are listed in Table 1 as  $\log \beta$ , where  $\beta$  is defined as

$$\beta_{qrs} = [\text{MH}_s]/[\text{M}][\text{H}]^s = \prod K_n \quad (1)$$

This table uses the nomenclature  $\text{M}_q\text{Cu}_r\text{H}_s$ , where  $q$ ,  $r$  and  $s$  represent the numbers of carbohydrate molecules

(ligands), metals and protons (negative values of  $s$  represent hydroxides) respectively in a complex.

The metal-binding constants of glucosamine hydrochloride, C2san hydrochloride and C4san hydrochloride were measured using a pH electrode with  $\text{KNO}_3$  as a supporting electrolyte. Typical solutions were 2.3 mM in ligand and between 1.9 and 1.0 mM in  $\text{Cu}(\text{NO}_3)_2$ . Plots of  $a$  versus  $\text{p}[\text{H}^+]$  showed an inflection at  $a > 2$ , 3 and 5 for  $\text{MH}^+$ ,  $\text{MH}_2^{2+}$  and  $\text{MH}_4^{2+}$  respectively, indicating the ready dissociation of all amino protons and the C(1) hydroxyl proton in the presence of Cu(II). The  $a$  versus  $\text{p}[\text{H}^+]$  curves for ligand and ligand/copper were coincident below  $\text{p}[\text{H}^+] = 5$ , indicating that glucosamine, C2san and C4san do not form complexes with Cu(II) in acidic media. The buffer region was extended past  $a = 2$ , 3 and 5 for the mono-, di- and tetrasaccharides respectively. The extended buffer region is indicative of the formation of hydroxide species. The equilibria of the chitosan mono-, di- and tetrasaccharides with copper are described in Scheme 1. Conditional stability constants are listed in Table 1 as  $\log \beta$ , where  $\beta$  is defined as

$$\beta_{qrs} = [\text{M}_q\text{Cu}_r\text{H}_s]/[\text{M}]^q[\text{Cu}]^r[\text{H}]^s \quad (2)$$

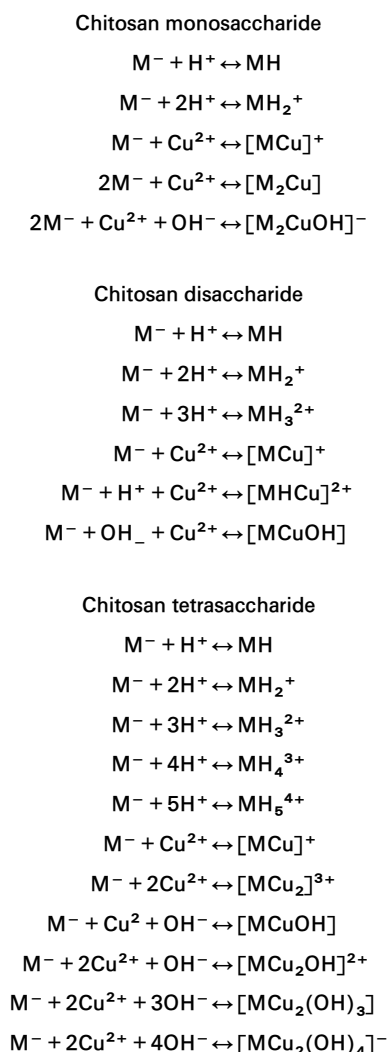
A systematic potentiometric study of the glucosamine oligomers shows that they do not behave like simple amines. In the case of glucosamine hydrochloride the C(1) hydroxyl is sufficiently acidic, owing to the inductive effect of the ether and amine, to dissociate a proton and act as an alkoxide ligand. In contrast, titrations of D(+)glucose and N-acetyl-D-glucosamine with hydroxide solution were also conducted in both the presence and absence of Cu(II). These studies demonstrated no evidence of proton dissociation or complex formation, indicating that the  $\text{pK}_a$  of the hydroxyl groups was greater than that of water. By inference we can conclude

**Table 1.** Conditional stability constants for chitosan monosaccharide, disaccharide and tetrasaccharide<sup>a</sup>

Species $\text{M}_q\text{Cu}_r\text{H}_s$ $q \ r \ s$			Log $\beta$		
			Monosaccharide	Disaccharide	Tetrasaccharide
1	0	1	13.13	13.47	13.54
1	0	2	20.75	21.06	21.23
1	0	3		27.57	28.25
1	0	4			34.75
1	0	5			40.50
$\sigma_{\text{fit}}$			0.01	0.03	0.01
1	1	0	10.98	12.97	13.41
2	1	0	20.33		
2	1	-1	8.57		
1	1	1		19.42	20.22
1	1	1		5.88	6.47
1	2	0			16.46
1	2	-1			10.02
1	2	-3			-1.92
1	2	-4			-10.50
$\sigma_{\text{fit}}$			0.01	0.02	0.01

<sup>a</sup>  $\text{M}_q\text{Cu}_r\text{H}_s$  represents the carbohydrate ligands M with the associated metals Cu and protons H. The subscripts  $q$ ,  $r$  and  $s$  refer to the numbers of ligands, metals and protons respectively in the complex. Negative values of  $s$  represent hydroxides.  $\sigma_{\text{fit}}$  is the goodness of fit of the refined stability constants.





**Scheme 1.** Solution equilibria for chitosan mono-, di- and tetra-saccharides with Cu(II).

that among the saccharides studied, only the C(1) hydroxyl of glucosamine can co-ordinate to copper via an alkoxide bond. Co-ordination of glucosamine is through the amine nitrogen and the C(1) alkoxide to produce a five-membered ring. A second glucosamine can co-ordinate in the same fashion to produce the neutral bisglucosamine complex. Additionally, at sufficiently high  $p[\text{H}^+]$ , co-ordination of a hydroxyl anion to the bisglucosamine complex is observed. The solution speciation of Cu(II) with glucosamine hydrochloride as a function of  $p[\text{H}^+]$  is shown in Fig. 6.

C2san hydrochloride can act as a tridentate ligand, co-ordinating to copper via an alkoxide and two amine moieties. Three distinct complexes were observed. The first to form was  $\text{MCuH}$ , where co-ordination is through the two amine nitrogens. At higher  $p[\text{H}^+]$  the C(1) hydroxyl is deprotonated, allowing C2san to act as a tridentate ligand to produce  $\text{MCu}$ . Co-ordination of a hydroxyl anion results in the formation of the neutral complex  $\text{MCuOH}$ .

C4san hydrochloride can act as a pentadentate ligand in a fashion analogous to that of C2san. Like C2san, C4san forms complexes with Cu(II) which have metal:ligand ratios of 1:1 ( $\text{MCuH}$ ,  $\text{MCu}$  and  $\text{MCuOH}$ ). In contrast with glucosamine and C2san,

C4san is also able to form complexes with 2:1 metal:ligand ratios. Significant quantities of  $\text{MCu}_2(\text{OH})_3$  and  $\text{MCu}_2(\text{OH})_4$  are present in solution at  $p[\text{H}^+] > 7$ . The species  $\text{MCu}_2(\text{OH})_4$  is particularly interesting in that the stoichiometry suggests a bridging hydroxyl anion between the metal centers of the complex. The solution speciation of C2san and C4san with Cu(II) as a function of  $p[\text{H}^+]$  is shown in Figs 7 and 8 respectively.

The potentiometric studies demonstrate that Cu–C4san complexes are principally neutral or negatively charged at  $p[\text{H}^+] = 7$ , explaining the absence of metal species in the positive ion ESI spectrum. Neutral metal complexes can be observed by ESMS if they can be converted to ionic species by one of several methods, such as protonation, metallation, electrochemical oxidation, conversion to quaternary cationic derivatives or chemical reaction.<sup>6</sup> To test the possibility of observing the neutral Cu–chitosan complex by converting it to an ionic species via association of the alkali metal cation with saccharide hydroxyl groups, NaI, KI or LiI was added to the copper–C4san solutions. No cationized Cu–C4san complexes were observed when solutions 40  $\mu\text{M}$  in C4san, 200  $\mu\text{M}$  in copper nitrate and 50–200  $\mu\text{M}$  in a selected alkali salt were electrosprayed.

A second approach examined for generating charge complexes was by collisionally heating the molecules to improve desolvation and induce fragmentation. This was achieved by increasing the voltage difference between the nozzle and the tube lens in the Finnigan ES interface,  $\Delta V$ . Whether desolvation, molecular dissociations of charge transfer/charge reduction reactions occur in the expansion region is determined by the magnitude of  $\Delta V$  and the nature of the analyte. Samples of 50  $\mu\text{M}$  chitosan with 200  $\mu\text{M}$  copper nitrate were thus analyzed under low-voltage ( $\Delta V = 20$  V) and high-voltage ( $\Delta V = 80$  V) conditions. The main species detected under low-voltage conditions was the doubly protonated C4san,  $[\text{M} + 2\text{H}]^{2+}$  ( $m/z$  332), shown earlier in Fig. 4. The high-voltage conditions resulted in formation of glycosidic cleavage products ( $m/z$  502, 341), dehydration reaction products ( $m/z$  323, 484) and Cu–C4san complexes ( $m/z$  724, 725 and 760) (Fig. 9). The observed intensities for the singly protonated C4san,  $[\text{M} + \text{H}]^+$  ( $m/z$  663), were also higher under high-voltage conditions, possibly owing to improved S/N under these conditions (Fig. 9).

The species at  $m/z$  760 corresponds to  $[\text{M} + \text{CuCl}]^+$  ( $662 + 63 + 35$ ), although an overlapping interference at  $m/z$  762 distorts the expected isotopic distribution pattern for  $[\text{M} + \text{CuCl}]^+$ . Commercial C4san is a hydrochloride salt; hence chloride ions are always present in the sample, associated with the amine groups. The  $[\text{C4san} + \text{CuCl}]^+$  complex could have originated from the droplet solution by protonation of a neutral  $[(\text{C4san} - \text{H})^-(\text{Cu})^{2+}(\text{Cl})^-]^0$  complex. This complex would be isoelectronic with a species, observed in potentiometric studies, in which the Cu(II) ion is co-ordinated to the C(1)-alkoxide, the four amine nitrogens of C4san and a hydroxyl anion. During potentiometric studies, solutions were not specifically probed for the presence of chloride-containing complexes; however, such species are not expected to form in the presence of high nitrate concentrations (0.1 M). In the ES samples,

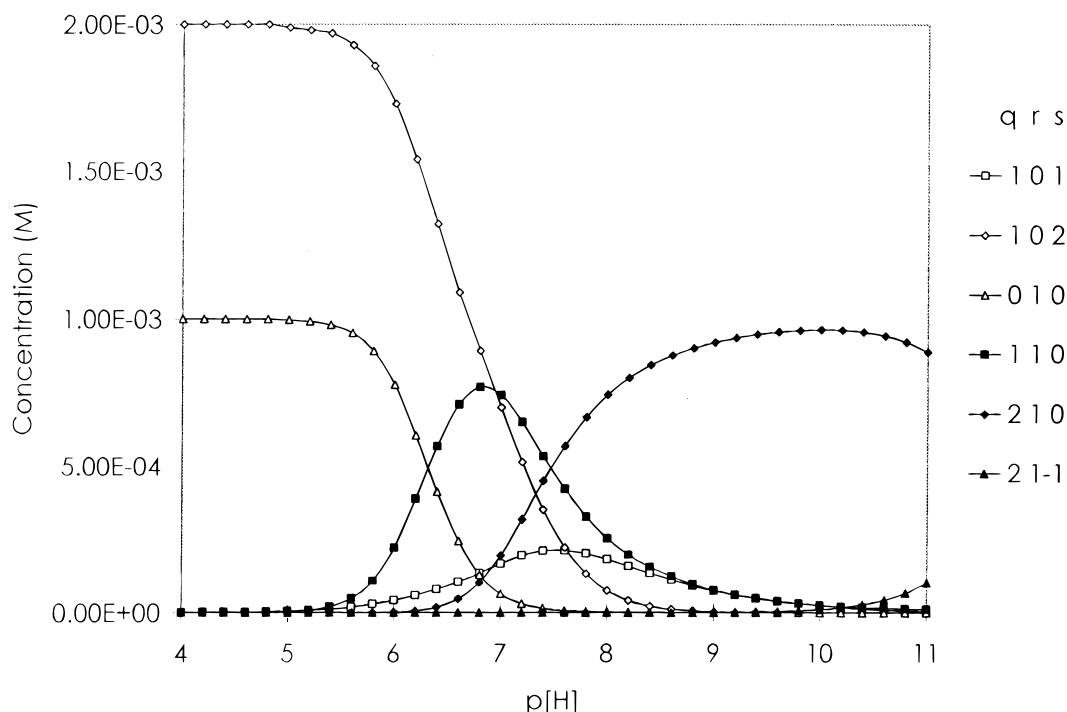


**Figure 6.** Calculated solution speciation of Cu(II) with glucosamine hydrochloride as a function of  $p[H^+]$ . The values  $q$ ,  $r$  and  $s$  refer to the numbers of ligands, metals and protons respectively in the complex. Negative values of  $s$  represent hydroxides.

however, chloride ion levels are similar to nitrate levels, hence the formation of neutral  $[C4san-Cu-Cl]$  complexes is plausible.

In fact, in a separate experiment, chloride ions were removed from the chitosan samples using strong anion exchange SPE cartridges (Supelco, Bellefonte, PA) that were dosed with nitrates. An ES sample 50  $\mu$ M in

C4san nitrate and 200  $\mu$ M in copper nitrate was then prepared and electrosprayed under both low- and high- $\Delta V$  conditions. The species with  $m/z$  760 could not be detected in this sample. The Cu-C4san species observed were  $m/z$  724, 725 and 787, the last of which corresponds to the nitric acid adduct. According to these experiments and in agreement with the poten-

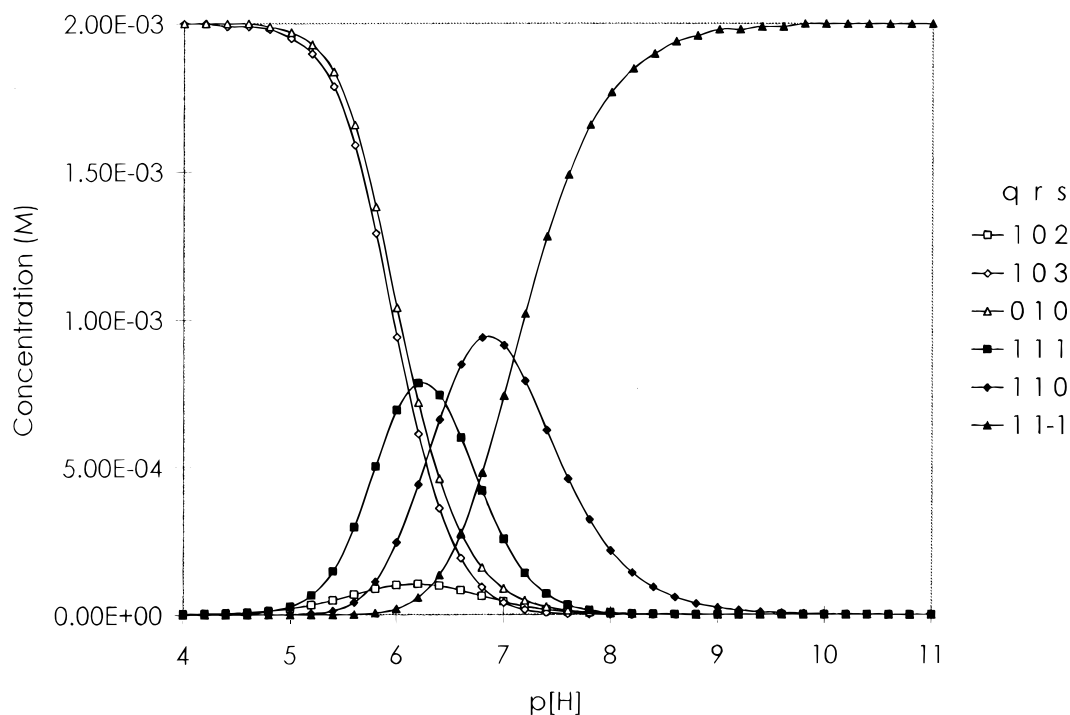


**Figure 7.** Calculated solution speciation of Cu(II) with chitosan disaccharide (C2san) as a function of  $p[H^+]$ . The values  $q$ ,  $r$  and  $s$  refer to the numbers of ligands, metals and protons respectively in the complex. Negative values of  $s$  represent hydroxides.

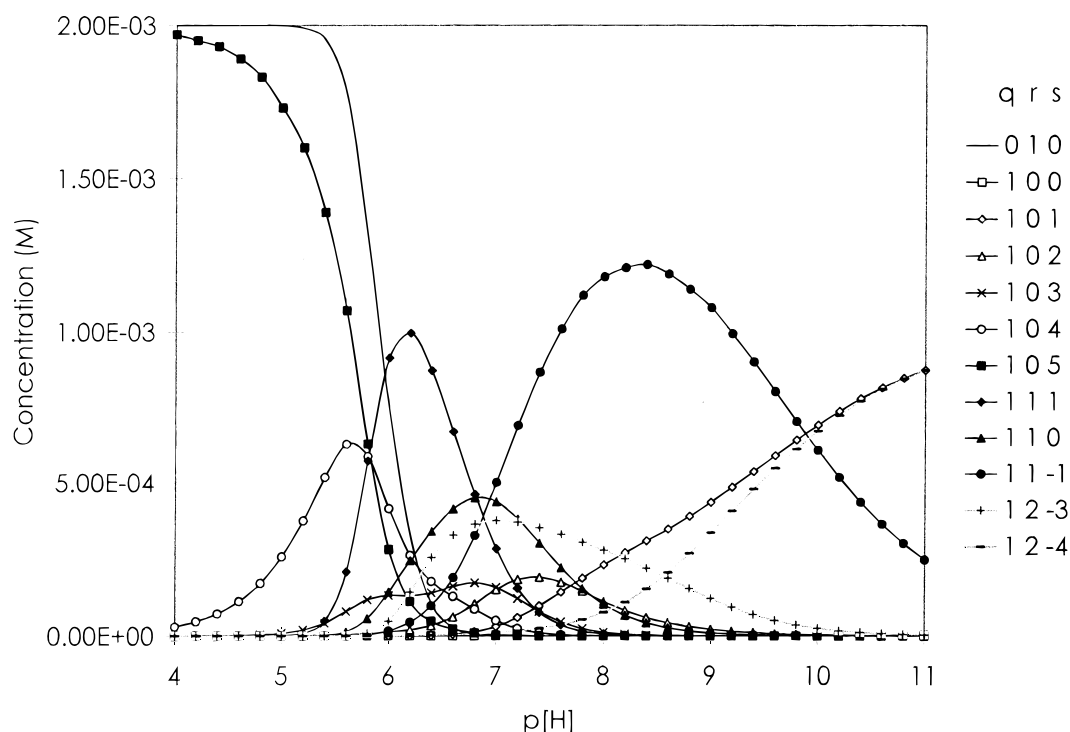


**Figure 8.** Calculated solution speciation of Cu(II) with chitosan tetrasaccharide (C4san) as a function of  $p[H^+]$ . The subscripts  $q$ ,  $r$  and  $s$  refer to the numbers of ligands, metals and protons respectively in the complex. Negative values of  $s$  represent hydroxides.

tiometric results, cupric ions and C4san appear to form a strong hexaco-ordinate complex in the condensed phase. In this complex the copper atom is co-ordinated to the four nitrogens, the C(1)-alkoxide moiety of C4san and an anion. The counter-ion is a chloride or nitrate in the ES samples.

Returning to the  $m/z$  760 species, it was further examined by CAD in the RF-only quadrupole of the TSQ-70 spectrometer (Fig. 10). Collisional activation of  $m/z$  760 resulted in loss of hydrochloric acid to form  $m/z$  724,  $[M - H + Cu]^+$ , glycosidic cleavage products of  $m/z$  724 ( $m/z$  563, 545, 402) and its cross-ring cleavage

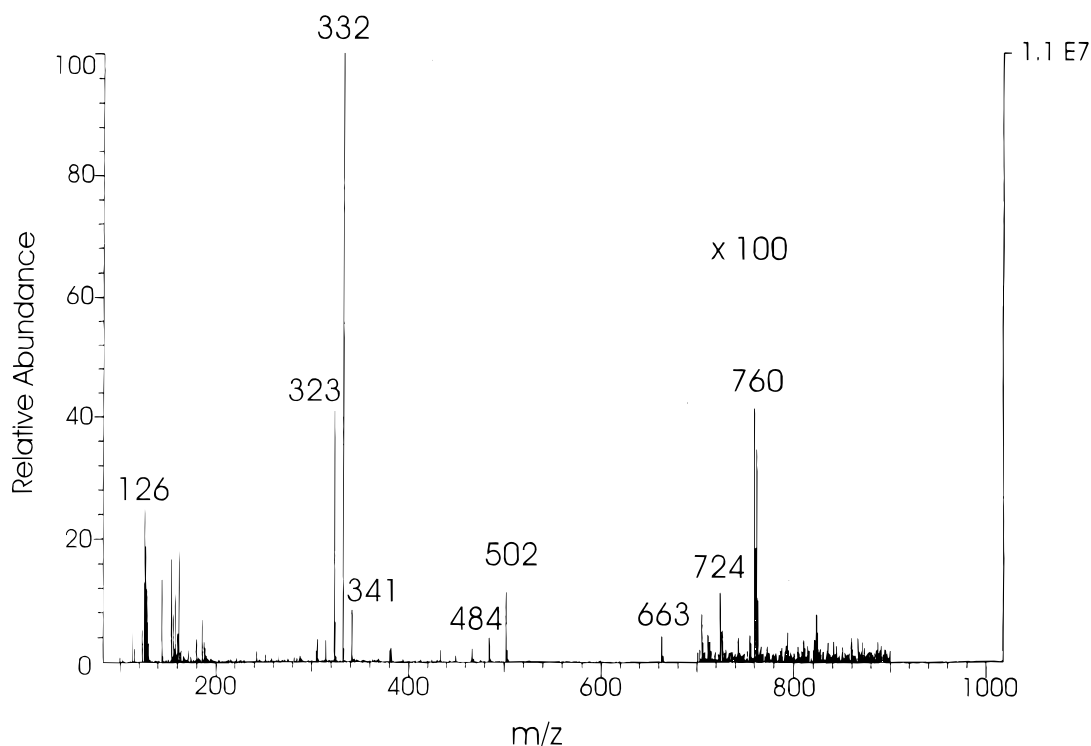


**Figure 9.** ES mass spectrum of 40  $\mu$ M chitosan tetrasaccharide and 200  $\mu$ M copper nitrate in 1:1 methanol:water under high-voltage conditions,  $\Delta V \approx 80$  V.  $\Delta V$  corresponds to the voltage difference between the heated capillary and the tube lens in the Finnigan electrospray interface.

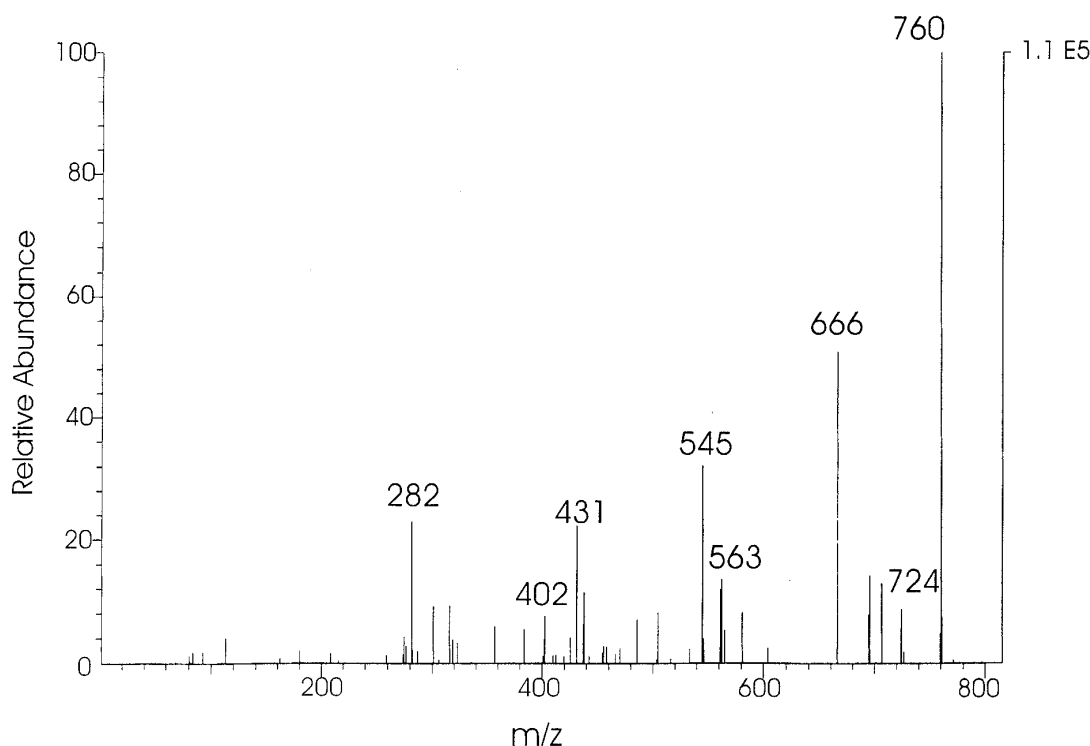


**Figure 10.** Collision-activated dissociation mass spectrum of copper-chitosan tetrasaccharide complex detected at  $m/z$  760 under high- $\Delta V$  conditions. Product ions  $m/z$  563, 545 and 402 are glycosidic cleavage ions of  $m/z$  724,  $[M - H + Cu]^+$ , formed by loss of hydrochloric acid from  $m/z$  760. Product ion  $m/z$  666 is a cross-ring cleavage ion of  $[M - H + Cu]^+$ ,  $m/z$  724. The ion  $m/z$  282 results from two neutral losses of 60 amu from  $m/z$  402. The signal at  $m/z$  431 was attributed to an impurity. Collision energies ranged between 20 and 40 V. Argon was the collision gas at a pressure of  $(2.4\text{--}2.6) \times 10^{-3}$  Torr.

product ( $m/z$  666). The product ion  $m/z$  282 represents a  $C_4H_8O_4$  neutral loss from  $m/z$  402, characteristic of  $\beta$ -1,4-linked saccharides.<sup>31</sup> The product ion  $m/z$  431 was attributed to an overlapping impurity, as determined by comparison with the CAD spectrum of  $m/z$  762, the higher-mass isotope of the copper-chitosan tetrasaccharide complex (Fig. 10). CAD of the latter ion,  $m/z$  762, resulted in a fragmentation pattern similar to that of  $m/z$  760, confirming the identity of this ion.

The appearance of the  $m/z$  760 ion under high-voltage conditions is partly due to the fourfold improvement in S/N, earlier attributed to improve ionic transmission and focusing under high- $\Delta V$  conditions. High- $\Delta V$  conditions also improve desolvation of electrosprayed species. Thus, if the protonated complex present in the droplets ( $[C4san + CuCl]^+$ ) had desorbed in highly solvated form, its observed abundance would increase under the high- $\Delta V$  settings which promote desolvation. In fact, raising the capillary temperature from 180 to 225 °C produced a similar effect, suggesting that the  $m/z$  760 ion was strongly solvated and required harsher conditions for its drying. Although the formation of the protonated complex ( $m/z$  760) by gas phase ion-molecule reactions cannot be completely discounted, again the low volatility of the neutral complex and high- $\Delta V$  conditions necessary to observe the protonated complex argue against gas phase reactions. A more likely explanation is that the neutral complex is protonated in the surface region of the droplet prior to or during desorption; high- $\Delta V$  conditions result in enough of an improvement in transmission and desolvation to allow observation of the

complex. This case again reflects a situation where the ESI spectrum cannot directly reflect solution chemistry (the complex is neutral), but a perturbation (protonation) during the desorption process allows the observation of the complex.

The observation of a protonated complex (e.g.  $m/z$  760) rather than a cationized species may be possibly related to the solution (droplet surface) conformation of the complex. Although the Lewis basicity of C4san hydroxyl groups is expected to decrease upon coordination with Cu(II), this is not expected to have a significant role in preventing the formation of cationized species. Thus failure to form a cationized species may indicate a more compact conformation for the Cu-C4san complex relative to free C4san, since the latter formed adducts with alkali ions but the former did not. The conformation of the Cu-C4san complex still allows association of smaller protons and formation of protonated  $[Cu-C4san-X]$  species (X signifies chloride or nitrate). However, this process is not very efficient, as demonstrated by their low-mass spectral abundances. The species with  $m/z$  724 appears to have resulted from dissociation of the protonated  $[Cu-C4san-X]$  complexes with the corresponding loss of HCl or HNO<sub>3</sub> rather than from direct desorption from solution.

The high- $\Delta V$  conditions also result in formation of very small amounts of a species with  $m/z$  725, corresponding to  $[M + Cu]^+$ . CAD of this ion also indicated glycosidic cleavage products ( $m/z$  564, 403) and a cross-ring cleavage product ( $m/z$  665) similar to those noted for the protonated  $[Cu-C4san-X]$  complex. Formation of the  $m/z$  725 ion under high- $\Delta V$  conditions

was attributed to reduction of copper in the singly charged complex  $[M + Cu^{2+}Cl^-]^+$  ( $m/z$  760), followed by a loss of a chloride radical ion to form  $[M + Cu]^+$ , consistent with Gatlin and Turecek's results with singly charged copper–amino acid complexes.<sup>39</sup>

Earlier it was mentioned that at  $p[H^+] > 7$  two additional copper–C4san complexes were formed in solution,  $MCu_2(OH)_3$  and  $MCu_2(OH)_4$ . Owing to high solution  $p[H^+]$  and difficulties with spray stability in the negative ion mode, these species were not explored mass spectrometrically.

## CONCLUSION

The associations between cupric ions and oligosaccharides of cellulose, chitin and chitosan were examined using potentiometry and electrospray mass spectrometry. The potentiometric data revealed no metal-binding affinities for mono- and tetrasaccharides of cellulose and chitin, while strong metal complexation was noted for mono- di- and tetrasaccharides of chitosan. These studies also demonstrated that the nitrogen atoms of chitosan tetrasaccharide and the C(1)-O were involved in formation of the co-ordination complexes in solution.

The ESMS results were more complex but generally seemed to indicate that solution equilibria were perturbed by droplet chemistry. For cellulose and chitin tetrasaccharides, several copper complexes were observed in spite of the absence of potentiometric evidence for these complexes in solution. These complexes were believed to have formed during desorption from the highly charged surfaces of the electrosprayed droplets. The complexes were observed under standard ES operating conditions, moderate capillary temperatures and moderate  $\Delta V$  and it seems unlikely that they were generated by gas phase reactions in the ES source. The relative abundances of the various copper–oligosaccharide species differed for the two saccharides and could partly reflect their conformations in the electrospray droplets.

In contrast with oligosaccharides of cellulose and chitin, the chitosan tetrasaccharide, C4san, formed strong complexes with cupric ions. The ESMS studies focused on observation of one of these complexes, the

most abundant species present at a pH of approximately 7. Under high- $\Delta V$  conditions, low abundances of protonated  $[Cu-C4san-X]$  (where X is chloride or nitrate) species were observed and these were further examined by CAD in the RF-only quadrupole of the triple-quadrupole mass spectrometer. These species were thought to have formed in solution ( $pH \approx 7$ ) as a neutral complex and subsequently become protonated in the shrinking ES droplets. Observation of small amounts of a charge-reduced product,  $m/z$  725, under high-voltage conditions was attributed to loss of a chloride radical from the singly charged complex,  $[M + Cu^{2+}Cl^-]^+$ , consistent with investigations of Gatlin and Turecek on singly charged copper–amino acid complexes.<sup>39</sup> The chitosan data appeared to reasonably reflect processes in solution even though the source operating parameters required careful adjustment before these complexes could be observed mass spectrometrically. It was believed that complexation of C4san to form a neutral solution complex reduced its ionization efficiency by preventing cation attachment, because the complexed conformation of C4san was more compact relative to that of the free form. None the less, protons were still capable of associating with this  $[Cu-C4san-X]$  complex to form cationic species, thereby allowing their desorption from the electrosprayed droplets.

The cellulose and chitin data were reasonable in light of the ion evaporation model<sup>38</sup> of electrospray and probably reflected processes in the highly charged electrospray droplets. The observed associations noted for cellulose and chitin appeared to be strictly governed by electrostatic interactions between cupric ions on the surface of the ES droplets and polar sites on the molecule to which charges (cupric ions) attached. The potentiometric results excluded the presence of any such associations between cupric ions and tetrasaccharides of cellulose and chitin in the bulk condensed phase. This is a clear example demonstrating the differences between electrospray spectra and solution equilibria.

## Acknowledgements

M. S., J. H. C. and B. J. R. acknowledge the support of the Office of Naval Research.

## REFERENCES

1. T. Midorikawa, E. Tanoue and Y. Sugimura, *Anal. Chem.* **62**, 1737 (1990).
2. G. A. Jackson and J. J. Morgan, *Limnol. Oceanogr.* **23**, 268 (1978).
3. D. M. Anderson and F. M. Morel, *Limnol. Oceanogr.* **23**, 283 (1978).
4. P. J. Wangersky, *Marine Chem.* **18**, 269 (1986).
5. (a) G. G. Geesey and L. Jang, in *Microbial Mineral Recovery*, ed. by Ehrlich and C. Rierly, p. 223. McGraw-Hill, New York (1990); (b) G. Geesey and L. Jang, in *Metal Ions and Bacteria*, ed. by T. Beveridge and R. Doyle, p. 325. Wiley, New York (1989); (c) G. Geesey and L. Jang, *Corrosion*, Paper 297. National Association of Corrosion Engineers, Boston, MA (1985).
6. (a) W. J. Cook and C. E. Bugg, in *Metal-Ligand Interactions in Organic Chemistry and Biochemistry*, Part 2, ed. by E. Pullman and N. Goldblum, pp. 231–256. Reidel, Dordrecht (1977); (b) R. Colton, A. D'Angostino and J. C. Traeger, *Mass Spectrom. Rev.* **14**, 79 (1995).
7. G. R. Agnes and G. Horlick, *Appl. Spectrosc.* **48**, 655 (1994).
8. (a) J. B. Fenn, M. Mann, C. K. Meng, S. F. Wong and C. M. Whitehouse, *Science* **246**, 64 (1989); (b) P. Kébarle and L. Tang, *Anal. Chem.* **65**, 972A (1993); (c) R. D. Smith, J. A. Loo, C. G. Edmonds C. J. Barinaga and H. R. Udseth, *Anal. Chem.* **62**, 882 (1990).
9. R. Colton, B. D. James, I. D. Potter and J. C. Traeger, *Inorg. Chem.* **32**, 2626 (1993).
10. (a) M. Barber, R. S. Bordoli, R. D. Sedgewick and A. N. Tyler, *J. Chem. Soc., Chem. Commun.* 325 (1981); (b) J. A. Sunner, A. Morales and P. Kébarle, *Int. J. Mass Spectrom. Ion Process.* **86**, 169 (1988); (c) G. Pelzer, E. De Pauw, D. Viet Dung and J. Marien, *J. Phys. Chem.* **88**, 5065 (1984).
11. (a) M. Vestal, *Anal. Chem.* **56**, 2590 (1984); (b) G. Schmelzeisen-Redeker, L. Butterling and F. W. Rollgen, *Int. J.*

- Mass Spectrom. Ion Process.* **90**, 139 (1989); (c) A. J. Alexander and P. Kebarle, *Anal. Chem.* **58**, 471 (1986).
12. (a) K. S. W. Chan and K. D. Cook, *J. Am. Chem. Soc.* **104**, 5031 (1982); (b) J. H. Callahan, K. Hool, J. D. Reynolds and K. D. Cook, *Anal. Chem.* **60**, 714 (1988).
13. J. C. Traeger, R. Colton and J. Harvey, *Org. Mass Spectrom.* **27**, 1030 (1992).
14. (a) P. Kebarle, P. Jayaweera, A. T. Blades and M. G. Ikonomou, *J. Am. Chem. Soc.* **112**, 2452 (1990); (b) A. T. Blades, P. Jayaweera, M. G. Ikonomou and P. Kebarle, *J. Chem. Phys.* **92**, 5900 (1990); (c) A. T. Blades, P. Jayaweera, M. G. Ikonomou and P. Kebarle, *Int. J. Mass Spectrom. Ion Process.* **102**, 251 (1990); (d) A. T. Blades, P. Jayaweera, M. G. Ikonomou and P. Kebarle, *Int. J. Mass Spectrom. Ion Process.* **101**, 325 (1990).
15. Z. L. Cheng, K. W. M. Siu, R. Guevremont and S. S. Berman, *J. Am. Soc. Mass Spectrom.* **3**, 281 (1992).
16. X. Yu. M. Wojciechowski and C. Fenselau, *Anal. Chem.* **65**, 1355 (1993).
17. P. Hu. Q. Ye and J. A. Loo, *Anal. Chem.* **66**, 4190 (1994).
18. G. J. Van Berkel, S. A. McLuckey and G. L. Glish, *Anal. Chem.* **63**, 1098 (1991).
19. C. Gatlin, F. Turecek and T. Valsar, *Anal. Chem.* **66**, 3590 (1994).
20. J. A. Loo and P. Hu, *J. Am. Chem. Soc.* **117**, 11314 (1995).
21. A. Van Dorsselaer, M. Jaquinod, E. Leize, N. Potier, A. M. Albrecht and A. Shanzer, *Tetrahedron Lett.* **34**, 2771 (1993).
22. R. A. A. Muzzarelli, *Chitin*. Pergamon, Oxford (1977).
23. C. D. Zamuda, D. A. Wright and R. A. Smucker, *Marine Environ. Res.* **16**, 1 (1985).
24. B. M. Sanders, K. D. Jenkins, W. G. Sunda and J. D. Costlow, *Science*, **222**, 53 (1983).
25. R. M. Brown Jr., I. M. Saxena and K. Kudlicka, *Trends Plant Sci.* **1**(5), 149 (1996).
26. S. J. Angyal, *Adv. Carbohydrate Chem. Biochem.* **47**, 1 (1989).
27. J. B. Fenn, *J. Am. Soc. Mass Spectrom.* **4**, 524 (1993).
28. A. E. Martell and R. J. Motekaitis, *Determination and Use of Stability Constants*. VCH, New York (1992).
29. D. D. Perrin and I. G. Sayce, *Talanta* **14**, 833 (1967).
30. J. A. Loo, H. R. Udseth and R. D. Smith, *Rapid Commun. Mass Spectrom.* **2**, 207 (1988).
31. E. M. Sible, S. P. Brimmer and J. A. Leary, *J. Am. Soc. Mass Spectrom.* **8**, 32 (1997).
32. B. G. Ershov, A. F. Seliverstov, N. L. Sukhov and G. L. Bykov, *Bull. Russ. Acad. Sci.—Div. Chem. Sci.* **41**, 1805 (1993).
33. (a) M. Shahgholi and J. H. Callahan, *Proceedings of the 42nd ASMA Conference on Mass Spectrometry and Allied Topics*, Chicago, IL, 1994, p. 1007; (b) M. Shahgholi, M. M. Ross and J. H. Callahan, *Proceedings of the 43rd ASMA Conference on Mass Spectrometry and Allied Topics*, Atlanta GA, 1995, p. 1185.
34. (a) A. Fura and J. A. Leary, *Anal. Chem.* **65**, 2805 (1993); (b) M. Kohler and J. A. Leary, *Proceedings of the 43rd Conference on Mass Spectrometry and Allied Topics*, Atlanta, GA, 1995, p. 1198; (c) M. Kohler and J. A. Leary, *Anal. Chem.* **67**, 3501 (1995).
35. X. Xu, S. P. Nolan and R. B. Cole, *Anal. Chem.* **66**, 119 (1994).
36. M. G. Ikonomou, A. T. Blades and P. Kebarle, *Anal. Chem.* **62**, 957 (1990).
37. S. J. Angyal, *Aust. J. Chem.* **25**, 1957 (1972).
38. J. V. Iribarne and B. A. Thomson, *J. Chem. Phys.* **64**, 2287 (1976).
39. (a) C. L. Gatlin and F. Turecek, *J. Mass Spectrom.* **30**, 1605 (1995); (b) C. L. Gatlin and F. Turecek, *J. Mass Spectrom.* **30**, 1617 (1995).
40. L. Tang and P. Kebarle, *Anal. Chem.* **65**, 3654 (1993).